journal

J. Am. Ceram. Soc., 87 [3] 352–57 (2004)

Metal–Urea Complex—A Precursor to Metal Nitrides

Yu Qiu and Lian Gao*,†

State Key Lab of High Performance Ceramics and Superfine Microstructure, Shanghai Institute of Ceramics, Chinese Academy of Sciences, Shanghai 200050, People's Republic of China

A novel and general route to synthesize various metal nitrides (AlN, CrN, and ζ-Fe_2N) from metal–urea complexes is presented. These complexes, especially metal–urea chloride, have proved to be useful precursors to metal nitrides, because urea molecules construct a coordination sphere around the metal atom and form a stable structure, compared with the air-sensitive halide. Different anions in the second coordination sphere determine the reaction mechanism. The transformation from metal–urea chloride to nitride is thought to follow a nucleation–growth mechanism, while that from metal–urea nitrate is thought to follow a nitridation mechanism. We anticipate that this metal–urea complex will find applications in the fabrication of other, more complex, nitrides.

I. Introduction

METAL NITRIDES are promising materials, because they have a wide variety of excellent properties, such as high hardness, good wear resistance, high melting point, high-temperature stability, high thermal conductivity, and large magnetization values, as well as good electrical and optical properties. For example, aluminum nitride (AlN) is used as an important ceramic substrate material because of its high thermal conductivity (170–260 $W\cdot m^{-1}\cdot K^{-1}$ for hexagonal- (*h*-) AlN and 250–600 $W\cdot m^{-1}\cdot K^{-1}$ for cubic- (*c*-) AlN).[1] AlN also is known as a piezoelectric material with a high acoustic velocity and as a refractory compound that resists oxidation.[2] Chromium nitride (CrN) shows a paramagnetic to antiferromagnetic transition at 280 K and has been identified as an excellent coating material because of its stability, high hardness, high melting point, and high wear resistance.[3,4] Iron nitride (FeN_x) has attracted extensive research interest for a long time because of its superior magnetic properties as well as improvement in the corrosion and abrasion resistance of materials surfaces.

Many processing methods used to synthesize metal nitride have been reported in recent literature, such as direct nitridation of the element,[5,6] oxide[7] and halide routes,[8] plasma-based processes,[9,10] and heat-treatment of organometallic precursors under ammonia gas.[11] Synthesis technologies should result in the production of materials that have optimum properties for performing specified functions. One of the most critical factors in the synthesis of metal nitrides is the starting material. There is increasing interest in developing alternative chemical approaches to metal nitrides using tailored molecular precursors, to lower the growth temperature, and to achieve molecular control over the crystal growth and the processing of the materials. Numerous efforts have been focused on organometallic compounds. However, the applications of organometallic compounds have been limited, because they are expensive, toxic, extremely unstable (even explosive), and very difficult to synthesize and handle. It is very desirable to develop a method that uses inexpensive precursor materials and is applicable to preparing various metal nitrides.

In this work, a novel route has been demonstrated that permits the simple and general synthesis of AlN, CrN, and Fe_2N from metal–urea complex precursors. An important synthesis step is the preparation of the metal–urea complex, which is a chemically stable and inexpensive compound, compared with other precursors, such as anhydrous chloride[12] or organometallic materials.[13,14] Urea replaces the coordinate water around the metal atom and decomposes at elevated temperatures, leaving metal chloride adducts with NH_3 (in the case of metal–urea chloride) or fine oxide particles (in the case of metal–urea nitrate) before the complex finally transforms to metal nitride under a flowing NH_3 atmosphere.

II. Experimental Procedure

(1) Materials and Processes

The starting chemicals used in this work were urea ($CO(NH_2)_2$, >99.0%), aluminum chloride ($AlCl_3\cdot 6H_2O$, >97%), aluminum nitrate ($Al(NO_3)_3\cdot 9H_2O$, >99%), chromium nitrate ($Cr(NO_3)_3\cdot 9H_2O$, >99%), iron(III) nitrate ($Fe(NO_3)_3\cdot 9H_2O$, >98.5%), anhydrous ethanol (C_2H_5OH, >99.5%), ammonia (NH_3, >99%), and nitrogen (N_2, >99.999%).

Metal chloride or nitrate was dissolved in anhydrous ethanol to obtain a concentrated solution. The solution then was added dropwise into a saturated urea/ethanol solution at 75°–80°C with stirring, until the final salt/urea molar ratio reached 1:6 (for chloride) or 1:9 (for nitrate). The reaction gave a water-soluble precipitate of a metal–urea complex, which was separated by filtration and dried at 80°C. The precipitate was characterized and used directly to synthesize metal nitrides without further purification. Some of the complex for each batch (5.0 g) was loaded into a quartz boat and heated under flowing NH_3 or N_2 (0.5 L/min) at 300°–1000°C for 1–15 h in a tube furnace to obtain metal nitrides. NH_3 gas was allowed to pass through the furnace for 1 h to remove the air in the furnace before the furnace was turned on, and the heating rate was kept at 10°C/min before it reached the set temperature. The resultant powder was collected after the furnace was cooled down under the flow of NH_3 gas. Similar procedures were conducted when high-purity N_2 was used. Table I summarizes the experimental conditions used.

(2) Characterization

The compositions of the metal–urea complexes were determined using chemical and elemental analysis (Model Vario EL, Elementar, Germany). The complex structures were characterized using Fourier-transform infrared spectroscopy (FTIR; Model NEXUS, Nicolet Instrument Corp., Madison, WI) and high-resolution solid-state ^{27}Al magic angle spinning and ^{13}C cross-polarization/magic angle spinning nuclear magnetic resonance (CP/MAS-NMR; Model Avance 300, Bruker Instruments, Inc., Billerica, MA) at room temperature. Simultaneous thermogravimetry–differential scanning calorimetry–mass spectroscopy (TG–DSC–MS; Model STA 449C, Netzsch, Bayern, Germany, and Model ThermoStar, Balzers, Liechtenstein) was used to record the

T. Parthasarathy—contributing editor

Manuscript No. 186486. Received December 16, 2002; approved October 20, 2003.

*Member, American Ceramic Society.
†Author to whom correspondence should be addressed.

Table I. Summary of Experiments on the Synthesis of Metal Nitride: Experimental Conditions and Results of XRD Analysis

Complex	Gas	Temperature (°C)	Time (h)	XRD phase[†]
AUC	NH_3	800	5	*h*-AlN > *c*-AlN
		800	8	*h*-AlN, *c*-AlN
		900	3	*h*-AlN > *c*-AlN
		900	5	*h*-AlN, *c*-AlN
		1000	5	*h*-AlN, *c*-AlN
	N_2	800	5	$(ClAlNH)_n^c$
CUN	NH_3	500	5	Cr_2O_3
		700	5	CrN > Cr_2O_3
		900	1	CrN > Cr_2O_3
		900	15	CrN
		1000	10	CrN >> Cr_2O_3[‡]
	N_2	700	5	Cr_2O_3 >> CrN
FUN	NH_3	300	3	Fe_2O_3
		500	5	ζ-Fe_2N > Fe_2O_3
		600	1	ζ-Fe_2N
	N_2	600	5	Fe_2O_3
AUN	NH_3	1000	8	α-Al_2O_3

[†]> is more than; >> is much more than. [‡]Characterized using FTIR.

thermal decomposition of aluminum–urea chloride under argon gas flow of 20 mL/min at a heating rate of 10°C/min.

The X-ray diffraction patterns of the synthesized products were obtained using powder X-ray diffractometry (XRD; Model D/Max 2550V, Rigaku, Tokyo, Japan) with Cu*K*α radiation (λ = 1.5406 Å). Scanning electronic microscopy (SEM; Model JSM-6700F, JEOL, Tokyo, Japan) and transmission electron microscopy (TEM; Model 200CX, JEOL) were performed to observe the microstructure of the products in selected cases.

III. Results and Discussion

(1) Characteristics of the Metal–Urea Complexes

Metal–urea complexes are water-soluble powders with various colors that depend on the metal salt used. Aluminum–urea chloride ($Al[OC(NH_2)_2]_6Cl_3$, AUC) and aluminum–urea nitrate ($Al[OC(NH_2)_2]_6(NO_3)_3$, AUN) are white powders, while chromium–urea nitrate ($Cr[OC(NH_2)_2]_6(NO_3)_3$, CUN) and iron-urea nitrate ($Fe[OC(NH_2)_2]_6(NO_3)_3$, FUN) are dark green and reddish brown powders, respectively. Measured and (calculated) chemical and elemental analyses are as follows: AUC, 5.59 (5.46) aluminum, 21.84 (21.54) chlorine, 14.56 (14.60) carbon, 33.52 (34.05) nitrogen, and 4.92 (4.90) hydrogen; CUN, 8.51 (8.69) chromium, 12.28 (12.04) carbon, 34.76 (35.11) nitrogen, and 4.10 (4.04) hydrogen; and FUN, 9.60 (9.27) iron, 12.11 (11.97) carbon, 34.08 (34.89) nitrogen, and 4.18 (4.02) hydrogen. FTIR spectra of AUC, CUN, and FUN are shown in Fig. 1, and the main bands in the infrared spectra are summarized in Table II. Through this assignment, particularly by the absence of a carbonyl band at 1684 cm^{-1},[15] and by the decrease in the wavenumber of the ν(CO) + $\delta(NH_2)$ vibration,[16] the formation of oxygen-to-metal coordinate bonds (C=O → M) in AUC, CUN, and FUN are determined.

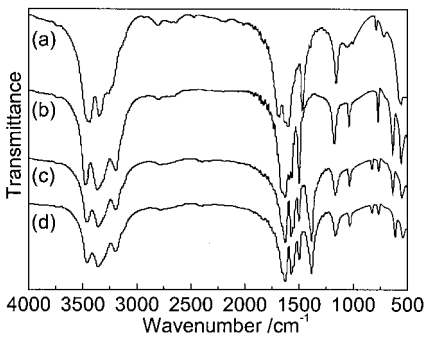

Fig. 1. Infrared spectra of (a) urea, (b) AUC, (c) CUN, and (d) FUN.

Table II. Absorption Maximums Observed for Urea and Metal–Urea Complexes and Their Assignments

Type of vibration	Observed frequency (cm^{-1})[†] Urea	AUC	CUN	FUN
$\nu_{as}(NH_2)$[15]	3435(s)	3473(s)	3460(s)	3460(s)
$\nu_s(NH_2)$[15]	3346(s)	3365(s)	3357(s)	3357(s)
Third N–H band[15]	3259(sh)	3192(m)	3195(m)	3197(m)
ν(CO)[15,16]	1684(s)	/	/	/
ν(CN) + $\delta(NH_2)$[16]	1628(sh)	1628(s)	1626(m)	1630(s)
ν(CO) + $\delta(NH_2)$[15,16]	1600(s)	1589(sh)	1572(s)	1572(s)
ν_{as}(CN)[15,17]	1468(s)	1498(s)	1498(m)	1498(m)
$\nu(NO_3^-)$	/	/	1385(s)	1385(s)
$\rho(NH_2)$[15,17]	1155(m)	1172(m)	1163(w)	1163(w)
ν_s(CN)[15,17]	1057(vw)	1036(m)	1032(w)	1030(w)
$\nu(NO_3^-)$	/	/	827(vw)	825(vw)
τ(ONCN)[17]	787(vw)	769(m)	764(vw)	766(vw)
δ(NCO)[15]	/	632(m)	634(w)	613(w)
δ(NCN)[15]	557(s)	557(m)	552(w)	544(w)

[†]s is strong, m is medium, w is weak, sh is shoulder, and / is not found.

To further confirm the structure of the metal–urea complexes, the ^{13}C CP/MAS-NMR and ^{27}Al MAS-NMR spectra of AUC were measured and found to have only one sharp resonance peak at δ of 161.7 ppm for ^{13}C NMR (Fig. 2(a)) and at δ of −7.6 ppm for ^{27}Al NMR (Fig. 2(b)). The ^{13}C peak is assigned for the carbon atoms in urea. The ^{27}Al peak corresponds to the octahedral AlO_6 coordinate bond, which proves the existence of oxygen-to-metal bonds. Meanwhile, the extremely narrow half-height width (42.5 Hz) of the ^{27}Al resonance peak shows a highly symmetrical structure. Thus, the structure of AUC (Fig. 3) can be expected according to the analysis above. Urea molecules locate in the first coordination

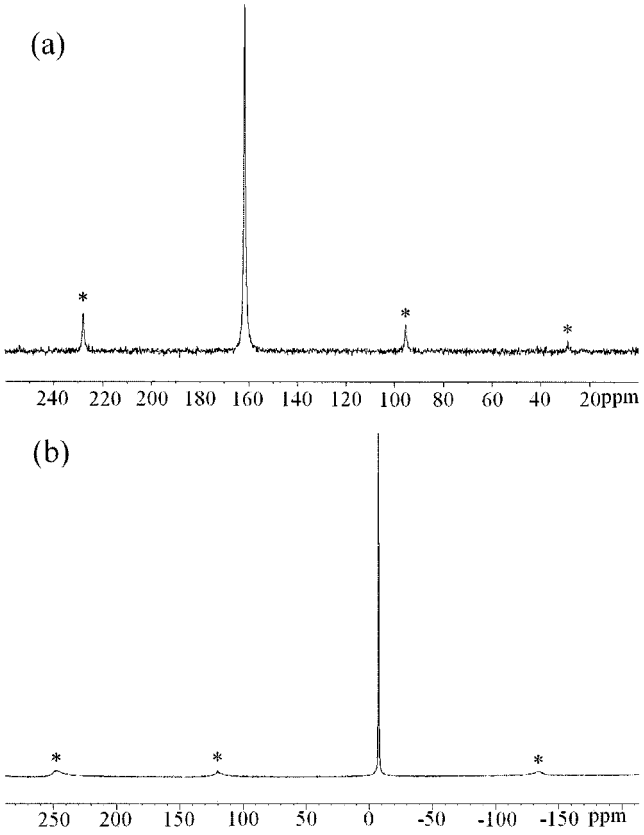

Fig. 2. (a) Solid-state ^{13}C CP/MAS-NMR and (b) ^{27}Al MAS-NMR spectra of AUC powder, operated at room temperature at 78.172 and 75.43 MHz, respectively. Spinning sidebands are denoted by an asterisk (*).

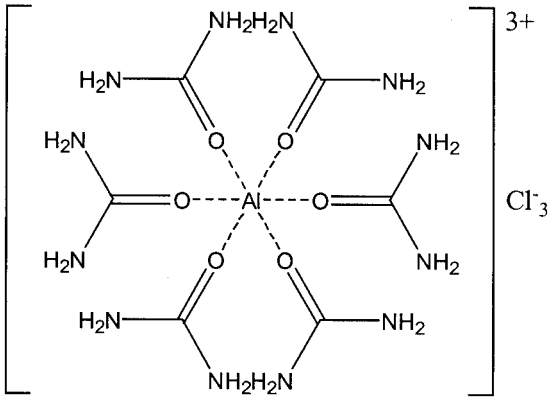

Fig. 3. Expected structure of AUC complex.

sphere near the aluminum atom, while the chloride anions locate in the outer coordination sphere. This structure stabilizes the vivid reactive $AlCl_3$ in an ambient atmosphere. Similar structures can be expected for CUN, FUN, and AUN.

(2) Thermal Behavior of the Metal–Urea Complex

AUC was analyzed using TG–DSC–MS to reveal the effect of the urea group during the decomposition of the complex. The TG–DSC curves of the thermal decomposition of AUC under argon atmosphere are shown in Fig. 4, and the temperature variation of the major species formed as determined using MS is shown in Fig. 5. Comparison of the TG and DSC curves leads to the conclusion that the diagrams contain very complicated thermal effects. The decomposition reaction takes place in three stages. The first stage starts at 180°C, with three fast and strong endothermic processes at 256°, 276°, and 305°C. The weight loss at the first stage is characterized as 63.3%, and the main decomposition products are identified by MS as NH_2, NH_3, HNCO, and H_2NCO (Fig. 5). The second stage is a weight loss (13.9%) between 350° and 650°C. The third stage is a moderate weight loss (15.5%) between 650° and 1000°C, which is accompanied by two endothermic peaks at ~818° and 930°C. In consistence with these two processes, the ion current intensity of HCl is detected to increase successively above 300°C. NH_3, NH_2, and H_2NCO also are detected in the last two stages. The thermal behavior is explained as follows.

(1) During the first stage, the complex decomposes to $AlCl_3$, according to Eq. (1) in Table III.[18] During the decomposition, a simultaneous degradation of urea takes place (Eqs. (2) and (3)).[16] Subsequently, $AlCl_3$ is converted to the $AlCl_3{\cdot}xNH_3$ adduct according to Eq. (4),[19] where x is determined as 3 using TG analysis.

(2) $AlCl_3{\cdot}NH_3$ forms when the temperature is >300°–400°C (Eqs. (5) and (6)),[19] which is unstable above 600°C. As the temperature increases, the elimination of HCl takes place (Eq. (7)) with simultaneous formation of more stable oligomeric $(Cl_2AlNH_2)_2$.[19,20]

(3) In the temperature range of 650°–1000°C, $(ClAlNH)_n$ forms.[2,21]

$(Cl_2AlNH_2)_2$ and $(ClAlNH)_6$ are the most important species in the chemical vapor deposition (CVD) process.[20] Our research results also prove that $(ClAlNH)_6$ and $(ClAlNH)_4$, with hexagonal and cubic geometry, respectively, are important in the formation of *h*- and *c*-AlN, which is discussed below. Jegier *et al.*[22] also have proposed a solid ($(HGaNH)_n$) remains after the heat-treatment of $(H_2GaNH_2)_3$. The further decomposition of $(ClAlNH)_n$ leads to AlN, which involves the elimination of HCl.[23] The reaction in this process is presented as Eqs. (8)–(10) in Table III. The decomposition process of AUC is more complicated than proposed above: the $AlCl_3$ and NH_3 decompose, and other species, such as Cl_2AlNH_2, ClAlNH, and oligomeric $(ClAlNH)_n$ (n = 2, 3), form.[23] We have examined the resulting amorphous AlN powder after the pyrolysis at 800°C for 5 h under an inert N_2 atmosphere (see Table I). The infrared spectrum gives vibration bands of ν(NH) at 3429 cm^{-1},[24,25] of Al–N_2 absorption at 2160 cm^{-1},[26] of δ_{as}(NH) at 1628 cm^{-1},[16,24,25] and of others in the 1600–1300 cm^{-1} region,[26] i.e., ν(AlN) at 719 cm^{-1},[25,27,28] and ν(AlCl) at 570 cm^{-1}.[25,29] This band assignment is evidence of intermediate solid compounds $(Cl_2AlNH_2)_2$ and $(ClAlNH)_n$ (n = 4, 6) in the reaction. When NH_3 is used as the carrier gas, the decomposition behavior is even more complicated. Weight losses and possible reactions during the decomposition of AUC are listed in Table III.

In the case of metal–urea nitrate, the thermal decomposition behavior is quite different from metal–urea chloride. Because of the presence of the vigorous oxidizing group NO_3^- in the outer coordination sphere of the complex besides the reducing urea group in the inner coordination sphere, fine oxide particles are formed after decomposition (Table I). The thermal decomposition of FUN under air has been studied by Carp *et al.*,[16] and their conclusion is further confirmed by our present study of CUN and FUN. Both studies give oxide as the major phase under an inert N_2 atmosphere. The transformations of CUN and FUN are discussed below.

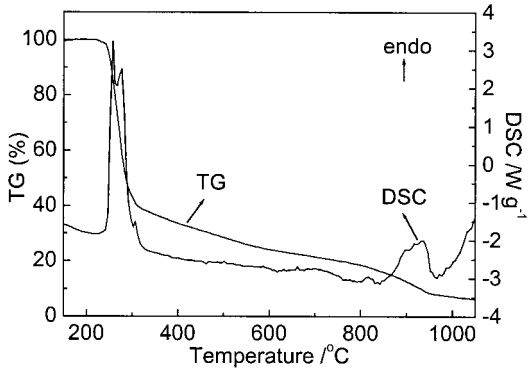

Fig. 4. TG and DSC curves of AUC at a heating rate of 10°C/min.

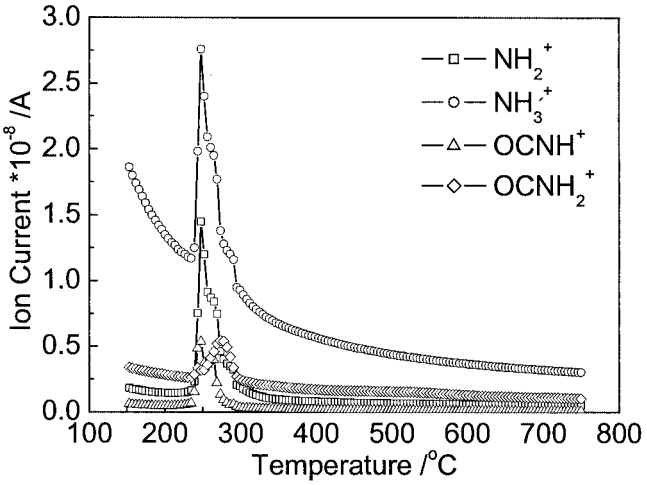

Fig. 5. Ion current intensity curves of AUC recorded using MS.

(3) Synthesis Mechanisms of Metal Nitrides

The metal nitrides, including *h*- and *c*-AlN, CrN, and ζ-Fe_2N, are derived from the thermal treatment of the metal–urea complexes under a flowing NH_3 atmosphere. Figure 6 shows the XRD patterns of metal nitrides obtained under various reaction conditions. Nanocrystalline AlN can be synthesized at 800°C, which is

Table III. Weight Loss and Possible Reactions during Thermal Decomposition of AUC under Argon

Temperature range (°C)	Weight loss (%)†	Possible reactions
150–350	63.3 (62.64)	(1) $Al[OC(NH_2)_2]_6Cl_3 \rightarrow AlCl_3 + 6CO(NH_2)_2$
		(2) $CO(NH_2)_2 \rightarrow NH_3 + HNCO$
		(3) $CO(NH_2)_2 \rightarrow NH_2 + H_2NCO$
		(4) $AlCl_3 + xNH_3 \rightarrow AlCl_3{\cdot}xNH_3$ ($x = 3$)
350–650	13.9 (14.28)	(5) $AlCl_3{\cdot}3NH_3 \rightarrow AlCl_3{\cdot}2NH_3 + NH_3$
		(6) $AlCl_3{\cdot}2NH_3 \rightarrow AlCl_3{\cdot}NH_3 + NH_3$
		(7) $AlCl_3{\cdot}NH_3 \rightarrow \frac{1}{2}(Cl_2AlNH_2)_2 + HCl$
650–1000	15.5 (14.77)	(8) $\frac{1}{2}(Cl_2AlNH_2)_2 \rightarrow \frac{1}{n}(ClAlNH)_n (n = 4, 6) + HCl$
		(9) $\frac{1}{4}(ClAlNH)_4 \rightarrow c\text{-}AlN + HCl$
		(10) $\frac{1}{6}(ClAlNH)_6 \rightarrow h\text{-}AlN + HCl$

†Measured and (calculated).

lower than the traditional chemical routes (usually >1200°C). The AlN synthesized under NH_3 is a mixture of hexagonal and cubic phases, with particle sizes mostly <25 nm, as observed using TEM (Fig. 7(a) and (b)). The cubic phase increases with increases in temperature or prolonged reaction time, and the amount is almost equal to that of the hexagonal phase when the temperatures is >800°C or the heating time is 8 h. The broadening of the XRD peaks makes it difficult to separate cubic (311) and (440) from hexagonal (101) and (103) peaks; therefore, selective area diffractometry (SAD) is used (Fig. 7 inset) and the results support the increase of *c*-AlN with temperature. The intensities of the (311), (400), and (440) planes of *c*-AlN become apparently much stronger under higher temperature. This result is notable, because *c*-AlN is an unstable phase at a high temperature. Timoshkin *et al.*[20] have concluded that, in CVD of AlN from $AlCl_3{\cdot}NH_3$, the preferable route is $(Cl_2AlNH_2)_2 \rightarrow c\text{-}(ClAlNH)_4$ or $h\text{-}(ClAlNH)_6 \rightarrow AlN$, wherein the formation of $(ClAlNH)_6$ is thermodynamically favored. That route is the possible reason why *h*-AlN is easier to prepare. In the present study, the formation of $c\text{-}(ClAlNH)_4$ cluster, which is the basic unit for the growth of *c*-AlN, may be thermally favored under heating conditions, according to the reaction[20]

$$\frac{1}{2}(ClAlNH)_6 \rightarrow \frac{1}{2}(ClAlNH)_4 \qquad \Delta H(298.15) = 51.7\ kJ{\cdot}mol^{-1}$$

The assembly of $(ClAlNH)_n$ ($n = 4, 6$) cluster to corresponding *c*- or *h*-AlN nucleus produces nanocrystalline AlN, which is a process similar to the nucleation–growth mechanism.

The decomposition of CUN and FUN gives mainly metal oxide under NH_3 atmosphere, before the nitridation of oxide by NH_3 gas, as revealed by the XRD analysis (Table I). In the nitridation process, the reaction temperature is the most important parameter for FUN, which fully converts to Fe_2N at 600°C (Fig. 6(c)), while the reaction time is the most important parameter for CUN, which needs a rather prolonged reaction time (15 h) for its complete conversion, even at a temperature as high as 900°C (Fig. 6(b)). This result can be explained by the stronger affinity of chromium atom to oxygen atom. The shifts of δ(NCO) and δ(NCN) to higher frequency are the evidences of a stronger O → Cr coordinate bond. The typical morphology of CrN and Fe_2N observed using SEM is presented in Figs. 8(a) and (b), respectively. SEM shows that the synthesis process produces porous, spongelike materials that contain fine nitride particles and large holes and voids. TEM clearly shows the nitride particles are angular and <1 μm, with smooth edges, which indicates good crystallization. Holes and voids are produced by gas that is released during the decomposition. These nitride materials are porous and have a high surface area, and they can be used as the matrix materials for composite materials or carrier materials for catalysts. Their morphology is distinct from that of AlN, which indicates a synthesis mechanism different from that of AUC. Different anions in the outer coordination sphere result in different decomposition and transformation mechanisms. To prove this assumption, AUN has been prepared and studied. AUN transforms to $\alpha\text{-}Al_2O_3$ after it is heated at 1000°C for 8 h (Table I), which results in the same morphology as that of Fe_2N and CrN.

Consequently, the formation of metal nitride from metal–urea chloride and nitrate can be assumed following two different mechanisms: (I) nucleation–growth and (II) nitridation, which are schematically represented in Fig. 9.

In mechanism I, the formation of AlN nanoparticles includes four steps: decomposition, formation of AlN monomers (single molecule in gas phase), nucleation, and growth of AlN particles. AUC decomposes to intermediate compounds $(ClAlNH)_n$ ($n = 4$,

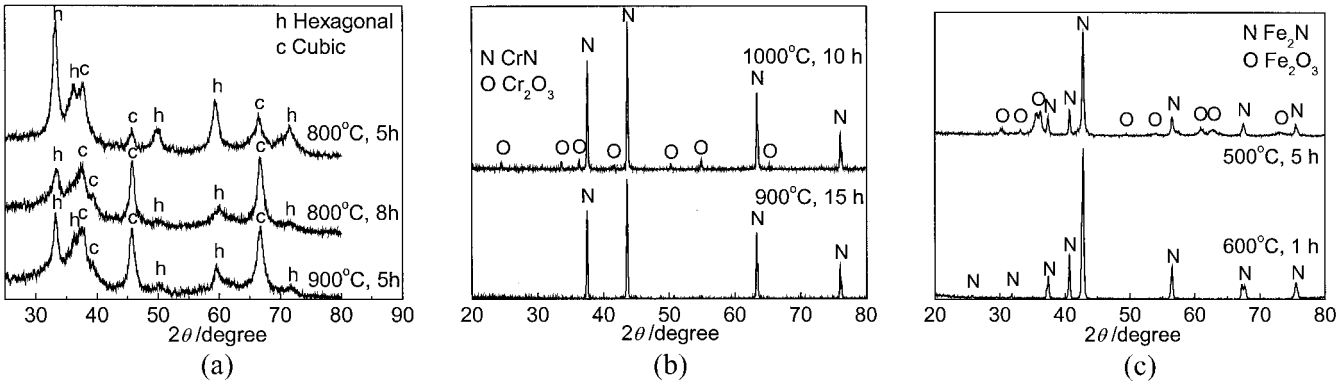

Fig. 6. Powder XRD patterns of (a) AlN, (b) CrN, and (c) Fe_2N synthesized under various conditions.

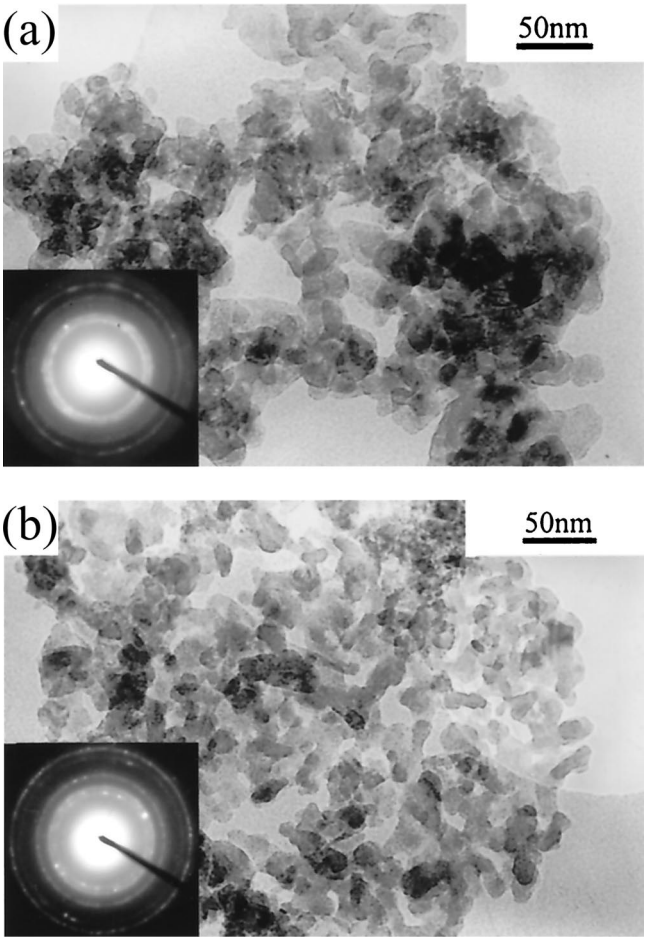

Fig. 7. TEM micrographs for the AlN powders synthesized at (a) 800° and (b) 900°C for 5 h. Insets are the associated SAD patterns. Innermost rings can be indexed to the *h*(100) plane, and the other rings from the inner to the outer can be indexed to *h*(002), *c*(311), *c*(222), *c*(400), *h*(110), *c*(440), and *h*(112).

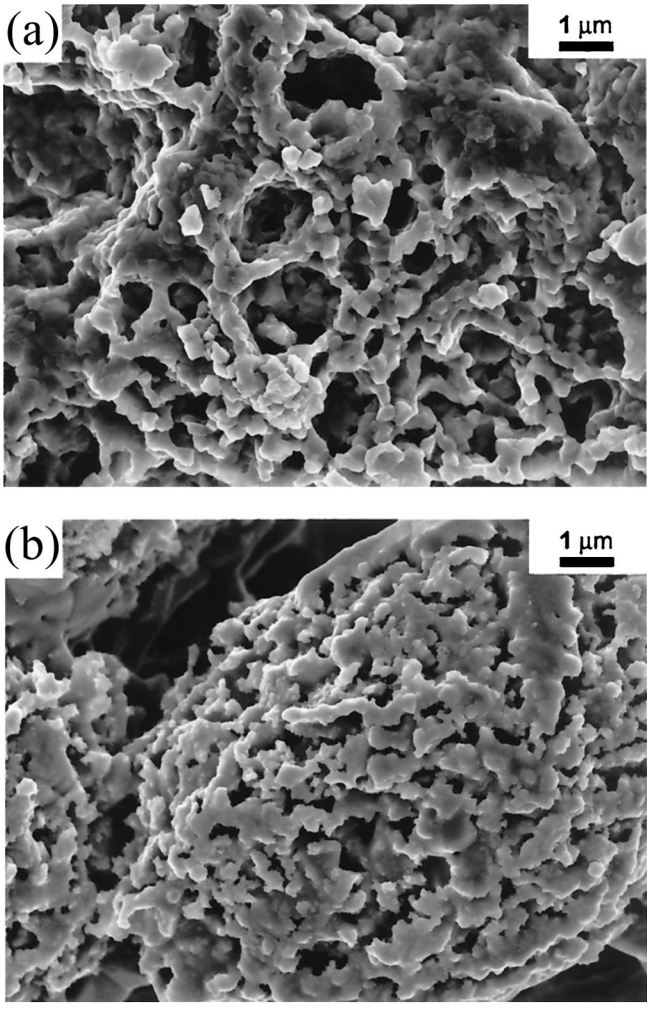

Fig. 8. SEM micrograph of (a) CrN synthesized at 900°C for 15 h and (b) Fe_2N synthesized at 600°C for 1 h.

6), which are the most important substances and the basic clusters (units) in this process. The formation of AlN molecules from $(ClAlNH)_n$ occurs via the elimination of HCl, with subsequent nucleation and growth processes. The decomposition of $AlCl_3{\cdot}NH_3$ adduct or the assembly of $(ClAlNH)_n$ can take place at the surface of the initial particles. Thus, the particle growth occurs through the following reactions.

(1) Surface reaction and elimination of HCl molecules:

$$AlCl_3{\cdot}NH_3\text{—}\mathbf{S} \rightarrow \tfrac{1}{n}(ClAlNH)_n\text{—}\mathbf{S} + 2HCl(g)$$

(2) Decomposition of intermediate solid compounds, assembly, or diffusion through the solid phase, and elimination of HCl molecules:

$$(ClAlNH)_n\text{—}\mathbf{S} \rightarrow nAlN(s) + nHCl(g)$$

where **S** is an adsorption or assembly site on the particle surface. In mechanism II, metal–urea nitrates first decompose to porous and unmethodical oxide powders. The oxide powders then react with NH_3 gas to form nitrides. It is concluded that the property of the anions in the outer coordination sphere of the complex results in the various reaction mechanisms.

IV. Conclusions

Two types of metal–urea complexes, metal–urea chloride and nitrate, are prepared as the starting materials for the synthesis of metal nitrides. The reductive urea group, which can degrade at a temperature >200°C, replaces the water molecule in the inner coordination sphere. AUC loses urea to yield oligomeric $(ClAlNH)_n$ (n = 4, 6), which can transform to nanocrystalline *c*- and *h*-AlN at elevated temperature under flowing NH_3 atmosphere through the nucleation–growth mechanism. Metal–urea nitrate decomposes mainly to fine oxide particles because of the presence of oxidative nitrate ion, and it further transforms to nitride by reacting with NH_3. It has been proved that metal–urea complex is a useful precursor to synthesize various metal nitrides. Metal–urea chloride, especially, is a good candidate for a precursor material to synthesize nanocrystalline metal nitride at a relatively low temperature. The metal–urea complex route appears to be very promising for elaboration of more complex nitrides.

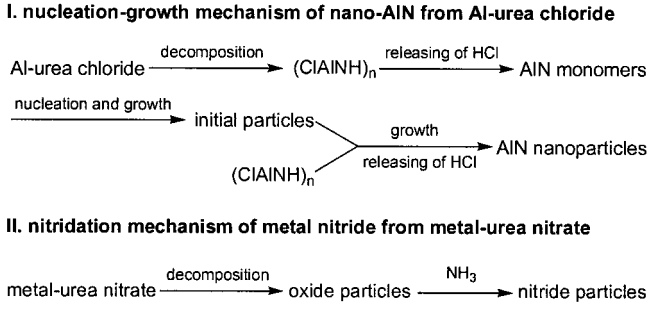

Fig. 9. Transformation mechanism from metal–urea complex to metal nitride.

References

[1]J. Wang, W. L. Wang, P. D. Ding, Y. X. Yang, L. Fang, J. Esteve, M. C. Polo, and G. Sanchez, "Synthesis of Cubic-Aluminum Nitride by Carbothermal Nitridation Reaction," *Diamond Relat. Mater.*, **8**, 1342–44 (1999).

[2]Y. Pauleau, A. Bouteville, J. J. Hantzpergue, and J. C. Remy, "Composition, Kinetics, and Mechanism of Growth of Chemical Vapor-Deposited Aluminum Nitride Films," *J. Electrochem. Soc.*, **129** [5] 1045–52 (1982).

[3]R. Ren, Z. Yang, and L. L. Shaw, "Synthesis of Nanostructured Chromium Nitrides through Mechanical Activation Process," *Nanostruct. Mater.*, **11**, 25–35 (1999).

[4]Z. Zhang, R. Liu, and Y. Qian, "Synthesis of Nanocrystallline Chromium Nitride from Ammonolysis of Chromium Chloride," *Mater. Res. Bull.*, **37**, 1005–10 (2002).

[5]J. A. Haber, P. C. Gibbons, and W. E. Buhro, "Morphological Control of Nanocrystalline Aluminum Nitride: Aluminum Chloride-Assisted Nanowhisker Growth," *J. Am. Chem. Soc.*, **119**, 5455–56 (1997).

[6]T. Yamaguchi, M. Sakita, M. Nakamura, and T. Kobira, "Synthesis and Characteristics of Fe_4N Powders and Thin Films," *J. Magn. Magn. Mater.*, **215–216**, 529–31 (2000).

[7]Y. Li, L. Gao, J. Li, and D. Yan, "Synthesis of Nanocrystalline Chromium Nitride Powders by Direct Nitridation of Chromium Oxide," *J. Am. Ceram. Soc.*, **85**, 1294–96 (2002).

[8]M. Cao, R. Wang, X. Fang, Z. Cui, T. Chang, and H. Yang, "Preparing of γ′-Fe_4N Ultrafine Powder by Twice-Nitriding Method," *Powder Technol.*, **115**, 96–98 (2001).

[9]H. D. Li, H. B. Yang, G. T. Zou, and S. Yu, "Ultrafine AlN and Al–AlN Powders: Preparation by dc Arc Plasma and Thermal Treatment," *Adv. Mater.*, **9** [2] 156–59 (1997).

[10]K. Niizuma and Y. Utsushikawa, "Synthesis of Fe–N Gradient Foil by Nitrogen Plasma," *Vacuum*, **59**, 260–65 (2002).

[11]R. L. Puurunen, A. Root, P. Sarv, M. M. Viitanen, H. H. Brongersma, M. Lindblad, and A. O. I. Krause, "Growth of Aluminum Nitride on Porous Alumina and Silica through Separate Saturated Gas–Solid Reactions of Trimethylaluminum and Ammonia," *Chem. Mater.*, **14**, 720–29 (2002).

[12]I. Kimura, N. Hotta, H. Nukui, N. Saito, and S. Yasukawa, "Synthesis of Fine AlN Powder by Vapour-Phase Reaction," *J. Mater. Sci. Lett.*, **7**, 66–68 (1988).

[13]L. Maya, "Synthetic Approaches to Aluminum Nitride via Pyrolysis of a Precursor," *Adv. Ceram. Mater.*, **1** [2] 150–53 (1986).

[14]W. Rockensüβ and H. W. Roesky, "$AlH_3(NMe_3)_2$—A Useful Precursor to AlN," *Adv. Mater.*, **5** [6] 443–45 (1993).

[15]R. B. Penland, S. Mizushima, C. Curran, and J. V. Quagliano, "Infrared Absorption Spectra of Inorganic Coordination Complexes. X. Studies of Some Metal–Urea Complexes," *J. Am. Chem. Soc.*, **79**, 1575–78 (1957).

[16]O. Carp, L. Patron, L. Diamandescu, and A. Reller, "Thermal Decomposition Study of the Coordination Compound $[Fe(urea)_6](NO_3)_3$," *Thermochim. Acta*, **390**, 169–77 (2002).

[17]J. C. Dobrowolski, R. Kolos, J. Sadlej, and A. P. Mazurek, "Theoretical and IR-Matrix Isolation Studies on the Urea and Urea–D_4, –^{13}C, and –1,3-$^{15}N_2$ Substituted Molecules," *Vib. Spectrosc.*, **29**, 261–82 (2002).

[18]R. R. Keuleers, J. F. Janssens, and H. O. Desseyn, "Comparison of Some Methods for Activation Energy Determination of Thermal Decomposition Reactions by Thermogravimetry," *Thermochim. Acta*, **385**, 127–42 (2002).

[19]C. Li, L. Hu, W. Yuan, and M. Chen, "Study on the Mechanism of Aluminum Nitride Synthesis by Chemical Vapor Deposition," *Mater. Chem. Phys.*, **47** [2–3] 273–78 (1997).

[20]A. Y. Timoshkin, H. F. Bettinger, and H. F. Schaefer, "The Chemical Vapor Deposition of Aluminum Nitride: Unusual Cluster Formation in the Gas Phase," *J. Am. Chem. Soc.*, **119**, 5668–78 (1997).

[21]D. W. Lewis, "Properties of Aluminum Nitride Derived from $AlCl_3$·NH_3," *J. Electrochem. Soc.*, **117**, 978–82 (1970).

[22]J. A. Jegier, S. McKernan, and W. L. Gladfelter, "Poly(imidogallane): Synthesis of a Crystalline 2-D Network Solid and Its Pyrolysis to Form Nanocrystalline Gallium Nitride in Supercritical Ammonia," *Chem. Mater.*, **10**, 2041–43 (1998).

[23]R. Riedel, G. Petzow, and U. Klingebiel, "Characterization of AlN Powder Produced by the Reaction of $AlCl_3$ with Hexamethyldisilazane," *J. Mater. Sci. Lett.*, **9**, 222–24 (1990).

[24]R. L. Puurunen, A. Root, P. Sarv, S. Haukka, E. I. Iiskola, M. Lindblad, and A. O. I. Krause, "Growth of Aluminium Nitride on Porous Silica by Atomic Layer Chemical Vapour Deposition," *Appl. Surf. Sci.*, **165** [2–3] 193–202 (2002).

[25]H. S. Wu, X. H. Xu, C. J. Zhang, and Z. H. Jin, "Studies on the Vibrational Spectra and Chemical Bond of Cl_nAlNH_n and H_nAlNH_n (n = 1–3)," *Chin. J. Struct. Chem.*, **19** [5] 378–86 (2000).

[26]G. Ecke, G. Eichhorn, J. Pezoldt, C. Reinhold, T. Stauden, and F. Supplieth, "Deposition of Aluminium Nitride Films by Electron Cyclotron Resonance Plasma-Enhanced Chemical Vapour Deposition," *Surf. Coat. Technol.*, **98** [1–3] 1503–509 (1998).

[27]G. F. Cata, G. R. Lorenzo, J. A. Odriozola, and L. J. Alvarez, "Charge-Transfer Molecular Dynamics of Aluminium Nitride," *Chem. Phys. Lett.*, **356** [1–2] 127–32 (2002).

[28]X. P. Hao, M. Y. Yu, D. L. Cui, X. G. Xu, Y J. Bai, Q. L. Wang, and M. H. Jiang, "Synthesize AlN Nanocrystals in Organic Solvent at Atmospheric Pressure," *J. Cryst. Growth*, **242**, 229–32 (2002).

[29]M. I. Shilina, V. V. Smirnov, O. R. Perlovskaya, and T. N. Rostovshchikova, "Theoretical and Low-Temperature IR Spectroscopic Studies of Catalytic Complexes of Aluminum Chloride with Nitroalkanes and Nitrobenzene," *J. Mol. Catal. A: Chem.*, **158**, 495–98 (2000). □